Luminosity diagnostics

J. Wenninger
CERN, Geneva, Switzerland

Abstract

The luminosity is, together with the beam backgrounds, the most important collider parameter as seen by the physics experiments that are installed at a collider. This document will first present the definition of the luminosity and its dependence on beam and accelerator lattice parameters. Direct measurement techniques, based on low-angle Bhabha or hadron detection, will be presented and compared to indirect determinations from beam and accelerator parameters. Luminosity optimization by beam overlap scans will be discussed.

1 Definition of the luminosity

When a particle encounters a target or another beam there is a certain probability that the encounter produces a final state composed of various particles. The likelihood of the process is expressed by its cross-section σ which represents virtually the area over which the process occurs. The cross-section σ is a surface and is expressed in units of m^2. In nuclear and high-energy physics a more common unit is the barn (b), where $1\ \mathrm{barn} = 10^{-24}\ \mathrm{cm}^2$. Typical cross-sections for rare processes like Higgs and exotic particle production are in the range of pb (picobarns, $10^{-36}\ \mathrm{cm}^2$) to fb (femtobarns, $10^{-39}\ \mathrm{cm}^2$).

For two colliding beams the number of collisions per unit time interval (the event rate) that produce the final state of interest is proportional to the cross-section, but it also depends on how well the beams collide and how much beam there is in the collider. The luminosity $\mathcal{L}$ quantifies the performance of the collider and relates the cross-section to the event rate $\dot{N}$:

$$\dot{N} = \frac{\mathrm{d}N}{\mathrm{d}t} = \sigma\mathcal{L}\ . \tag{1}$$

Besides quantifying the collider performance, the luminosity is also needed to determine the cross-section for a process from the measured event rate. Typical demands on the accuracy on $\mathcal{L}$ range from the per mil to the few per cent level. The luminosity $\mathcal{L}$ is usually expressed in units of $\mathrm{cm}^{-2}\mathrm{s}^{-1}$. For modern colliders $\mathcal{L}$ lies in the range of 10^{28} to $10^{34}\ \mathrm{cm}^{-2}\mathrm{s}^{-1}$. The PEP-II and KEKB B-factories have achieved luminosities in excess of $10^{34}\ \mathrm{cm}^{-2}\mathrm{s}^{-1}$, and the LHC design luminosity is around $10^{34}\ \mathrm{cm}^{-2}\mathrm{s}^{-1}$.

The integrated luminosity $\mathcal{L}_{\mathrm{int}}$ and the total number of events N are obtained by integrating over time:

$$N = \sigma \int_{t_0}^{t_1} \mathcal{L}\mathrm{d}t = \sigma\mathcal{L}_{\mathrm{int}}\ . \tag{2}$$

Frequently $\mathcal{L}_{\mathrm{int}}$ is expressed in pb^{-1} ($10^{36}\ \mathrm{cm}^{-2}$) or fm^{-1} ($10^{39}\ \mathrm{cm}^{-2}$). For $\mathcal{L}_{\mathrm{int}} = 1\ \mathrm{pb}^{-1}$ a process with a cross-section of 1 pb yields one event (on average).

A collider with a luminosity of $10^{31}\ \mathrm{cm}^{-2}\mathrm{s}^{-1}$ that operates with an efficiency of 100% for 24 hours produces an integrated luminosity of

$$\mathcal{L}_{\mathrm{int}} = 8.6 \times 10^{35}\ \mathrm{cm}^{-2} = 0.86\ \mathrm{pb}^{-1}\ , \tag{3}$$

i.e., almost $1\ \mathrm{pb}^{-1}$. Integrated luminosities of the order of $1\ \mathrm{fm}^{-1}$ per day can be produced by the KEKB and PEP-II B-factories and by the LHC at its design luminosity of $10^{34}\ \mathrm{cm}^{-2}\mathrm{s}^{-1}$.

2 Luminosity and machine parameters

To better understand the concept of luminosity, it is useful to relate it to accelerator parameters. Intuitively the luminosity depends on:

- the number N of particles that collide;
- the distribution of the particles within the beams, usually characterized by the r.m.s. beam sizes σ_x, σ_y and σ_s where x, y and s label the horizontal, the vertical, and the longitudinal plane;
- the collision frequency that depends on the revolution frequency f and on the number of bunches k (for a bunched beam).

The general expression of the luminosity for two bunched beams (labelled 1 and 2) is [1]

$$\mathcal{L} = kfN_1N_2 \int \rho_1(x,y,s,t)\rho_2(x,y,s,t)\mathrm{d}x\mathrm{d}y\mathrm{d}s\mathrm{d}t \tag{4}$$

where $\rho_i(x,y,s,t)$ represents the density distribution of the particles of beam i. Here s is the longitudinal coordinate and t the time. In the absence of crossing angles, the distributions for beams with Gaussian profiles can be decomposed into

$$\rho(x,y,s,t) = \rho_x(x)\rho_y(y)\rho_s(s-ct) \tag{5}$$

where

$$\rho_u(u) = \frac{1}{\sigma_u\sqrt{2\pi}} \exp\left\{-\frac{(u-u_0)^2}{2\sigma_u^2}\right\}, \tag{6}$$

with c the speed of light and u_0 the offset of the beam position with respect to the origin of the coordinate system. When the expressions for ρ_u are substituted in Eq. (4) and integrated, one obtains the general expression for the luminosity of two beams with Gaussian profiles colliding without crossing angle:

$$\mathcal{L} = \frac{kfN_1N_2}{2\pi\sqrt{(\sigma_{x,1}^2+\sigma_{x,2}^2)(\sigma_{y,1}^2+\sigma_{y,2}^2)}} \exp\left\{-\frac{\Delta x^2}{2(\sigma_{x,1}^2+\sigma_{x,2}^2)} - \frac{\Delta y^2}{2(\sigma_{y,1}^2+\sigma_{y,2}^2)}\right\}, \tag{7}$$

where Δx and Δy are the offsets between the beams at the collision point for the horizontal and vertical plane. For beams of equal sizes, $\sigma_{u,i} = \sigma_u$, this expression can be simplified to

$$\mathcal{L} = \frac{kfN_1N_2}{4\pi\sigma_x\sigma_y} \exp\left\{-\frac{\Delta x^2}{4\sigma_x^2} - \frac{\Delta y^2}{4\sigma_y^2}\right\}. \tag{8}$$

From this expression for beams of equal size, one obtains the standard expression for the luminosity when the beams collide without offsets ($\Delta x = \Delta y = 0$) and without crossing angle:

$$\mathcal{L} = \frac{kfN_1N_2}{4\pi\sigma_x\sigma_y}. \tag{9}$$

For a separation of one σ in one of the two planes, for example $\Delta x = \sigma_x$, the luminosity reduction is $\exp(-1/4) = 0.78$ with respect to the peak luminosity for $\Delta x = 0$.

When the beams cross at an angle, as is frequently the case for modern high-luminosity colliders, see for example Fig. 1 and Fig. 2, the luminosity is reduced because the particles no longer traverse the entire length of the counter-rotating bunch. In the absence of transverse offsets, $\Delta x = \Delta y = 0$, the luminosity for a horizontal crossing angle is given by

$$\mathcal{L} = \frac{kfN_1N_2}{4\pi\sigma_x\sigma_y} \frac{1}{\sqrt{1+\left(\frac{\sigma_s}{\sigma_x}\tan(\phi/2)\right)^2}}, \tag{10}$$

where ϕ is the full crossing angle (i.e., the angle between the two beams). The luminosity degrades as the bunch length projection $\sigma_s \times \tan(\phi/2)$ becomes more important with respect to the transverse beam size. For example, at the LHC the luminosity reduction due to the 300 µrad crossing angle is $\approx 17\%$ for $\sigma_x = 16$ µm and $\sigma_s = 7.6$ cm.

In all equations that have been presented so far, it was implicitly assumed that the beam sizes are constant over the collision region. This is usually a good assumption, but for very strong focusing when the bunch length σ_s approaches or is smaller than the betatron function β^* at the collision point, the beam size may vary significantly over the length of the collision region, producing a so-called *hour glass* effect. In such a case a numerical integration of Eq. (4) may become necessary [1].

3 Evolution of luminosity measurements

The direct determination of the luminosity from beam and lattice parameters using the equations presented in the previous section is made at every collider, at least as a means to estimate the quality of the beam and lattice measurements (Section 4). It turns out that this simple method does not usually provide a sufficiently accurate luminosity measurement, in particular because the collision offsets that can easily affect the luminosity at the level of a few per cent are not easy to measure accurately and continuously while the beams collide. As a consequence, other techniques have been developed to provide an absolute luminosity measurement: S. Van de Meer devised a beam scan technique for the ISR to determine the absolute luminosity that is still in use more than 40 years after its development (Section 4.1).

For most accelerators, accurate measurements are obtained by monitoring a physics process that can be either computed theoretically with sufficient precision or calibrated during special calibration runs (Section 5). The Bhabha scattering process is used universally at all $\mathrm{e^+e^-}$ colliders for accurate measurements of the luminosity (Section 5.1). For hadron colliders the situation is more complicated because the theoretical computation of cross-sections for strong interaction is more delicate (Section 5.2). The use of the optical theorem that relates the cross-section to the scattering rates in the forward region to calibrate the luminosity was first used at the ISR. This technique involves special detectors that can be moved very close to the circulating beams in order to perform measurements at the smallest scattering angles. This technique will again be used at the LHC for the luminosity calibration (Section 5.3).

4 Luminosity determination from machine parameters

The a priori most evident way to determine the luminosity is to compute it from machine parameters:

- k and f are known to high accuracy.
- The number of particles per beam N (or alternatively the beam currents) can be measured to an accuracy level of 1% from a well calibrated beam current transformer.
- The beam sizes σ_u are more difficult to measure, since they cannot be determined at the collision point owing to the presence of the experiment. The beam size must be obtained from the beam emittance and from a measurement of the betatron function at the collision point. Dispersive contributions to the beam size may have to be taken into account as well. It is in general difficult to determine σ_u to better than 5–10% accuracy, in particular for $\mathrm{e^+e^-}$ colliders running at large beam–beam tune shifts.
- When the beams cross at an angle, the crossing angle ϕ must be determined with sufficient accuracy using nearby Beam Position Monitors (BPMs). Figure 1 shows the layout of an LHC collision point with BPMs installed in the vicinity of the collision point to extrapolate the beam positions and angles to the collision point.

Unless a special effort is made it is in general not evident to deduce the luminosity to better than 5–10% accuracy from the machine parameters. With special effort the accuracy can be reduced to a few per cent, in particular at hadron colliders where the beam–beam tune shift is not too large,

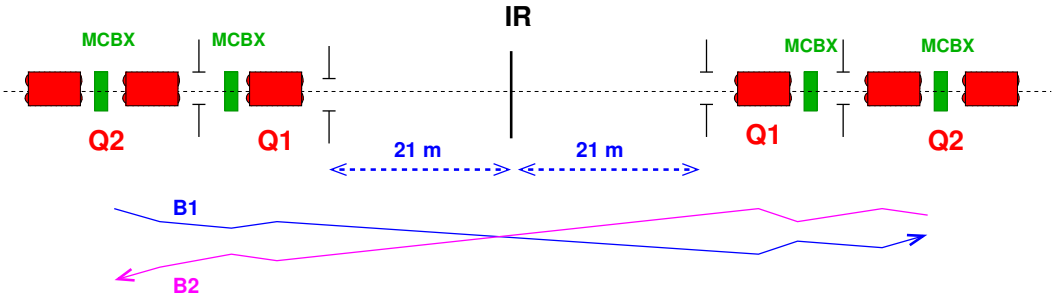

Fig. 1: Layout of an LHC collision point. The beams cross with an angle $\phi = 300$ µrad in either the horizontal or the vertical plane. BPMs are installed in the vicinity of the collision point to determine the crossing angle. The symbols B1 and B2 refer to the two beams.

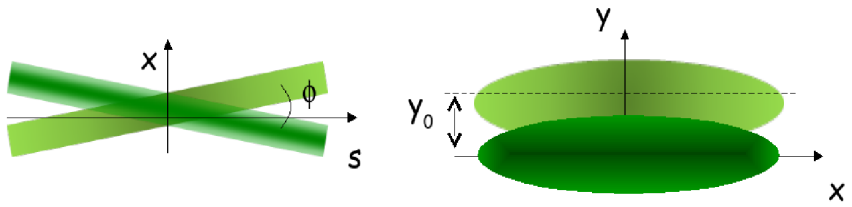

Fig. 2: Crossing angle and vertical separation scan at the ISR

4.1 Van de Meer scans

An elegant luminosity determination is based on an idea suggested by S. Van de Meer for the ISR where it was used to calibrate the luminosity measurement with an accuracy around 1%, as described in Refs. [2–4]. The ISR was colliding two coasting (unbunched) beams with a horizontal crossing angle. In such a configuration of coasting beams $\mathcal{L}$ does not depend on the horizontal beam offsets. $\mathcal{L}$ only depends on the vertical beam offset y_0, see Fig. 2, and may be expressed as

$$\mathcal{L}(y_0) = \frac{N_1 N_2 f^2 h_{\text{eff}}(y_0)}{c \tan(\phi/2)} \,, \tag{11}$$

where the effective height is given by

$$h_{\text{eff}}(y_0) = \frac{\dot{N}(y_0)}{\int \dot{N}(y_0) \mathrm{d}y_0} \,. \tag{12}$$

The principle is shown in Fig. 2 and Fig. 3. The beams must be scanned as a function of the vertical position y_0 and the reaction rate recorded for each separation setting. In the following sections we shall discuss ways to measure a reaction rate. The luminosity at the optimum setting can be determined from the normalized rate h_{eff} that does not depend on knowledge of the absolute cross-section. It is, however, necessary to have a bias-free rate measurement and the scale of the scan must be known to high accuracy. At the ISR the scale was calibrated with beam scrapers. Obviously such scans also provide the optimum setting for best beam overlap and highest luminosity.

For bunched beams the scans must be performed for each plane independently. As an illustration one can derive the general equation for a Van de Meer scan of beam with Gaussion profile based on Eq. (8). The reaction rate is proportional to the luminosity and to the beam offsets

$$\dot{N}(\Delta x, \Delta y) = \dot{N}_0 \exp\left\{ -\frac{\Delta x^2}{4\sigma_x^2} - \frac{\Delta y^2}{4\sigma_y^2} \right\} . \tag{13}$$

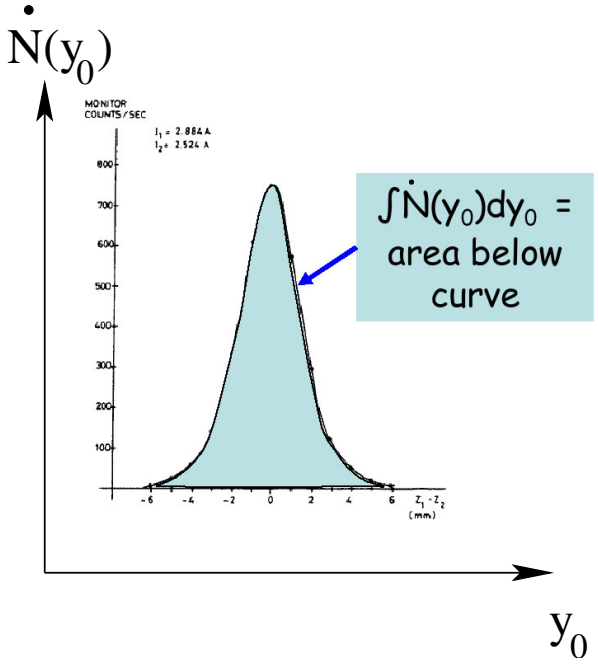

Fig. 3: Principle of the Van de Meer scan with the event rate as a function of the vertical beam separation. The luminosity is obtained from the ratio of the rate at a given separation y_0 to the integrated rate represented by the blue surface. It is not necessary to perform any absolute calibration of the rate.

For a scan of the vertical separation Δy the integrated rate over the scan is

$$\int \dot{N}(\Delta x, \Delta y)\mathrm{d}(\Delta y) = \dot{N}_0 \sqrt{4\pi}\sigma_y \exp\left\{-\frac{\Delta x^2}{4\sigma_x^2}\right\} \tag{14}$$

and the vertical effective height at the optimum separation ($\Delta y = 0$) is given by

$$h_{\mathrm{eff},y} = \frac{\dot{N}(\Delta x, 0)}{\int \dot{N}(\Delta x, \Delta y)\mathrm{d}(\Delta y)} = \frac{1}{\sqrt{4\pi}\sigma_y} \,. \tag{15}$$

For a horizontal scan with fixed vertical separation one obtains the horizontal effective height at the optimum separation ($\Delta x = 0$)

$$h_{\mathrm{eff},x} = \frac{\dot{N}(0, \Delta y)}{\int \dot{N}(\Delta x, \Delta y)\mathrm{d}(\Delta x)} = \frac{1}{\sqrt{4\pi}\sigma_x} \,. \tag{16}$$

When scanning in a given plane it is not necessary to be at the optimum setting for the other plane, since the effect of the offset in the orthogonal plane cancels out in h_{eff}. The effective height basically measures the beam size in the plane that is scanned. Equation (9) for peak luminosity may be re-expressed in terms of the effective heights:

$$\mathcal{L} = kfN_1N_2h_{\mathrm{eff},x}h_{\mathrm{eff},y} \,. \tag{17}$$

One of the main difficulties is the precise calibration of the scan scales, since this uncertainty enters directly in the luminosity error. Careful calibrations of the steering elements must be performed using response measurements, or the profiles must be calibrated accurately using beam halo scrapers as was done at the ISR.

Another potential complication arises for high beam–beam tune shift colliders like LEP or the B-factories where the beam size may vary significantly as a function of the beam separation during such a scan, thus biasing the results significantly.

5 Luminosity measurements from cross-sections

For a known or well calibrated physics process, the definition of the luminosity may be inverted such as to express the luminosity as a function of the cross-section and of the event rate:

$$\mathcal{L} = \frac{\dot{N}}{\sigma} \,. \tag{18}$$

To perform a good measurement of $\mathcal{L}$ it is necessary to find a physics process that satisfies the following criteria:

- The process is theoretically very well established and the cross-section σ can be computed with an adequate accuracy.
- The rate $\dot{N}$ is high to ensure a sufficient statistical accuracy (for a fast measurement) and can be measured experimentally with the desired accuracy.
- Background processes contributing to $\dot{N}$ are well known, can be experimentally identified, and their contribution can be subtracted.

5.1 Luminosity measurement at $\mathrm{e^+e^-}$ colliders

For linear or circular $\mathrm{e^+e^-}$ colliders the Bhabha scattering process is normally used for luminosity measurements:

$$\mathrm{e^+e^-} \longrightarrow \mathrm{e^+e^-}(n\gamma) \tag{19}$$

where γ is a photon. This process has a large cross-section and it is almost a pure electromagnetic interaction that may be computed from quantum electrodynamics (QED). At LEP the cross-section could be computed theoretically to an accuracy of better than 0.05% [5]. To enhance the rate and reduce contributions that do not arise from QED, the detector should be installed at a small angle to the beam. The cross-section for a detector covering the angular range from θ_{min} to θ_{max} is

$$\sigma \propto \{\frac{1}{\theta^2_{\mathrm{min}}} - \frac{1}{\theta^2_{\mathrm{max}}}\} \,. \tag{20}$$

At LEP each of the four experiments had a luminosity monitor covering the angular regions between $\theta_{\mathrm{min}} = 30$ and $\theta_{\mathrm{max}} = 50$–$100$ mrad. The detectors were installed on both sides of the collision points to detect both the outgoing electrons and positrons and to reduce the background with coincidence measurements. The detectors were usually composed of an electromagnetic calorimeter, based for example on scintillating crystals, and an accurate tracking detector based on silicon strip or pixel detectors to measure precisely the angle of the outgoing electrons and positrons. The experiments achieved measurement accuracies at the 0.1% level [6]. To reach such accuracies at small angles, the alignment of the detector is of extreme importance.

The LEP machine had its own detectors that were installed at smaller angles between 2 and 5 mrad to achieve faster update rates, see Fig. 4 and Ref. [7]. The detectors were composed of a sandwich of tungsten plates (to produce the electromagnetic showers) interleaved with silicon strip detectors to measure the position of the shower and the shower energy (Fig. 5). The absolute accuracy of the machine detector was poor and the detectors were calibrated with respect to their counterparts from the four LEP experiments. The machine monitors were used mainly for luminosity optimization as will be discussed later.

5.2 Luminosity measurement at (anti-)proton colliders

For the case of (anti-)proton beams, it is more difficult to find processes where the theoretical cross-section is well known. For the LHC (and also the Tevatron) the processes that can be used are [8, 9]

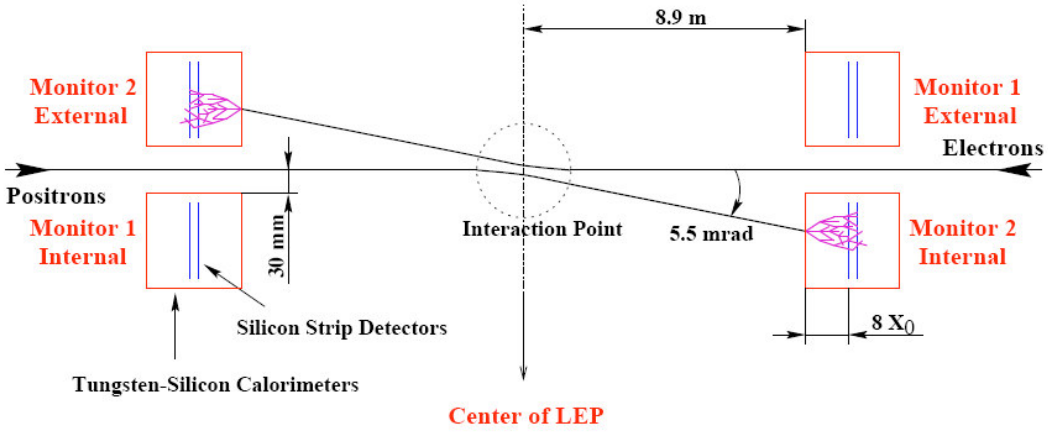

Fig. 4: Layout of the LEP machine luminosity monitors (from Ref. [7]). The e^+ and e^- pairs from Bhabha scattering are observed with coincidences from detectors on either side of the collision point.

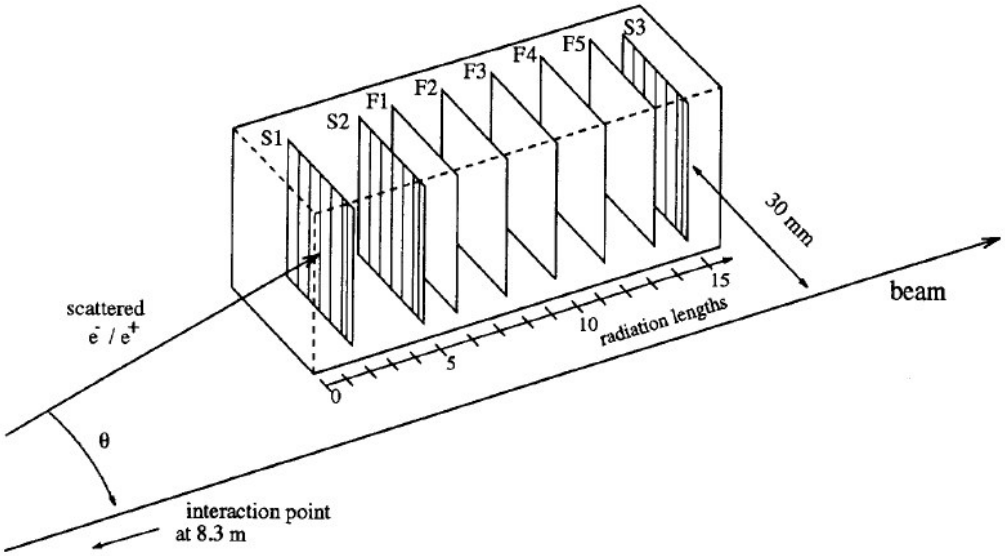

Fig. 5: Schematic drawing of the LEP machine luminosity monitor. Each detector consists of a sandwich of tungsten plane and silicon detectors. Some detectors consisted of 16 Si strips (labelled Sj) to determine the position of the shower, while others consisted of a single channel (labelled Fj) to measure the total signal. The radiation length of tungsten is 3.5 mm. The position of the shower maximum is around 6–7 radiation lengths.

– Lepton pair production

$$\mathrm{p} + \mathrm{p} \longrightarrow X + Y + l^+ l^- \tag{21}$$

where X, Y represent either a proton or a hadron jet and $l^+ l^-$ is a lepton pair (electron or muon).

– W or Z boson production

$$\mathrm{p} + \mathrm{p} \longrightarrow X + \mathrm{Z} \longrightarrow X + l^+ l^- \tag{22}$$

$$\mathrm{p} + \mathrm{p} \longrightarrow X + \mathrm{W} \longrightarrow X + l^{(+/-)} \nu \tag{23}$$

since the Z and the W may be identified by their decay into a lepton pair (Z) or a lepton and a neutrino (missing energy).

The processes are illustrated schematically in Fig. 6.

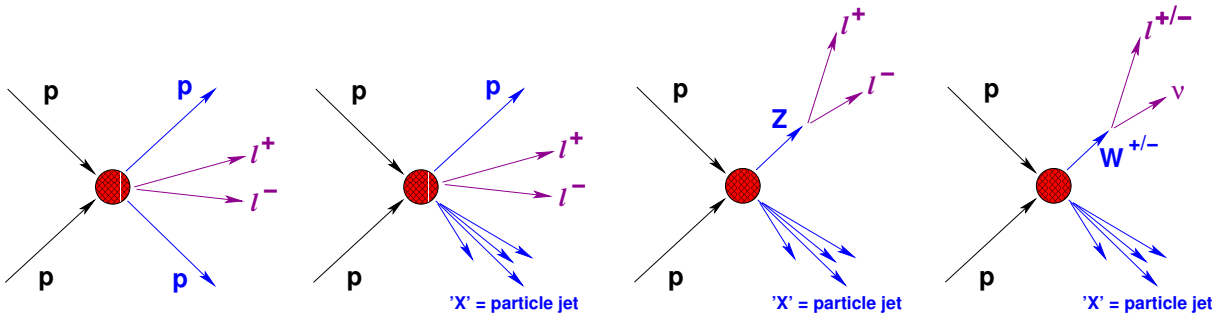

Fig. 6: Illustration of the processes that can be used in (anti-)proton–proton collisions to measure or monitor the luminosity: lepton (electron or muon) pair production l^+l^- and W/Z boson production. The incoming protons are shown on the left, the outgoing particles on the right. The interaction at the collision point is represented by the circle.

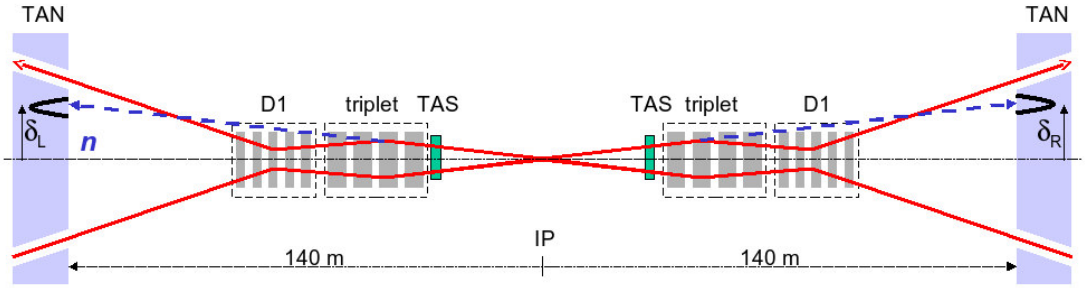

Fig. 7: Layout of the LHC interaction region where the two counter-rotating proton beams collide in a section of common vacuum chamber. The location indicated as IP corresponds to the collision point. The two beams are indicated by the red lines. The D1 dipole magnets are used to separate/recombine the two beams. Owing to the close bunch spacing of 25 ns, the beams must collide with a crossing angle. The neutral particles (neutrons, photons, neutral pions, etc.) that are produced at very small angle (basically along the beam directions) are absorbed in neutral particle absorbers (TAN) on either side of the collision point. The LHC luminosity detectors are installed inside the TAN absorbers.

In cases where only a relative luminosity measurement is of interest, it is sufficient to measure the particle rate at a small angle to ensure that the measurement is fast enough. The rate will be proportional to the luminosity, only the absolute calibration will not be known. At the LHC the machine luminosity monitors that are used to bring the beams into collisions and to optimize the beam overlaps are located in the very forward region. They are installed in the neutral particle absorber between the dipole magnets that separate and recombine the two beams around the collision point, see Fig. 7. At the two high-luminosity collision points of the LHC this location is highly radioactive with yearly integrated radiation doses above 100 MGy at nominal performance. The detectors must therefore be robust and survive many years of operation without any maintenance [10]. A very fast ionization chamber filled with argon gas was chosen as detector. At the two low-luminosity collision points (factor 100 or more lower luminosity) a fast detector based on CdTe crystals was selected [10].

5.3 Luminosity measurement at (anti-)proton colliders from the optical theorem

An alternative for protons is to measure the cross-section at very small angles and use the optical theorem that relates the total cross-section to the event rate in the forward direction:

$$\sigma = \frac{16\pi}{1+\rho^2}\frac{(\mathrm{d}R_{\mathrm{el}}/\mathrm{d}t)_{(t=0)}}{R_{\mathrm{el}}+R_{\mathrm{inel}}} = \frac{16\pi}{1+\rho^2}\frac{(\mathrm{d}R_{\mathrm{el}}/\mathrm{d}t)_{(t=0)}}{\dot{N}} \,. \tag{24}$$

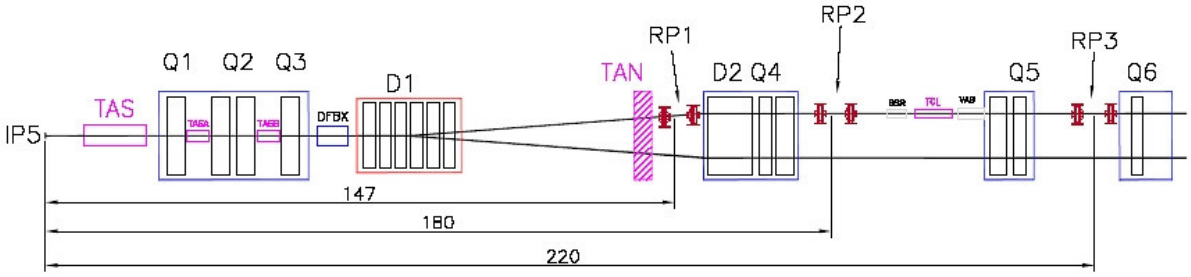

Fig. 8: Layout of the TOTEM experiment at the LHC, with detectors (*Roman Pots*, labelled RP_i, i = 1,2,3) installed between around 150 and 220 m from the collision point

In this context t represents the four-vector momentum transfer between the incoming and outgoing proton; ρ is the ratio of the real and imaginary part of the elastic nuclear scattering amplitude in the forward direction (zero angle); $\rho \approx 0.135$ [9, 11]. Here R_{el} is the event rate for elastic proton–proton collisions

$$\mathrm{p} + \mathrm{p} \longrightarrow \mathrm{p} + \mathrm{p} \tag{25}$$

while R_{inel} is the event rate for inelastic collisions

$$\mathrm{p} + \mathrm{p} \longrightarrow \mathrm{p} + X \tag{26}$$

and $\dot{N} = R_{\mathrm{el}} + R_{\mathrm{inel}}$. For elastic scattering of the protons with momentum P at an angle θ, the momentum transfer t is:

$$t = -2P^2(1 - \cos\theta) \cong -2P^2\theta^2 \; . \tag{27}$$

To determine the cross-section, both the total event rate as well as the elastic rate must be measured. The elastic rate must be extrapolated to the forward direction $t = 0$. To minimize the extrapolation errors, the scattering angles must be as small as possible. Such a measurement requires special detectors that can move very close to the beam to determine R_{el} at the smallest possible angles and momentum transfer, and minimize the errors due to the interpolation. Such detectors are nicknamed *Roman Pots* due to their pot-like shape. Such measurements have been performed at the ISR [12], Sp$\bar{\mathrm{p}}$S [13], the Tevatron and are foreseen for the LHC, see, for example, Ref. [11] for an overview of the results. At the LHC the measurements will be performed by TOTEM [14] (Fig. 8) and ATLAS [15]. The luminosity calibrations are performed under very special machine conditions and must be cross-calibrated with other detectors of the CMS and ATLAS experiments. A special optics with low divergence (and large-sized) beams at the collision points must be designed for such measurements [16]. In order to achieve the desired 1% accuracy, the detector alignment and systematic errors must be well controlled. The machine parameters (emittance, local optics, beam energy, etc.) must be determined and stabilized with very tight tolerances.

5.4 Luminosity measurement at ion colliders

At ion colliders the luminosity may be determined from the measurement of neutrons scattered in the forward direction with a precision of the order of 5% [17]. The neutrons are detected with so-called Zero Degree Calorimeters (ZDC). The ZDCs are designed to measure neutrons scattered in the very forward direction during ion beam collisions in two-ring colliders. Such detectors are in use at RHIC [18] and will be installed in the LHC.

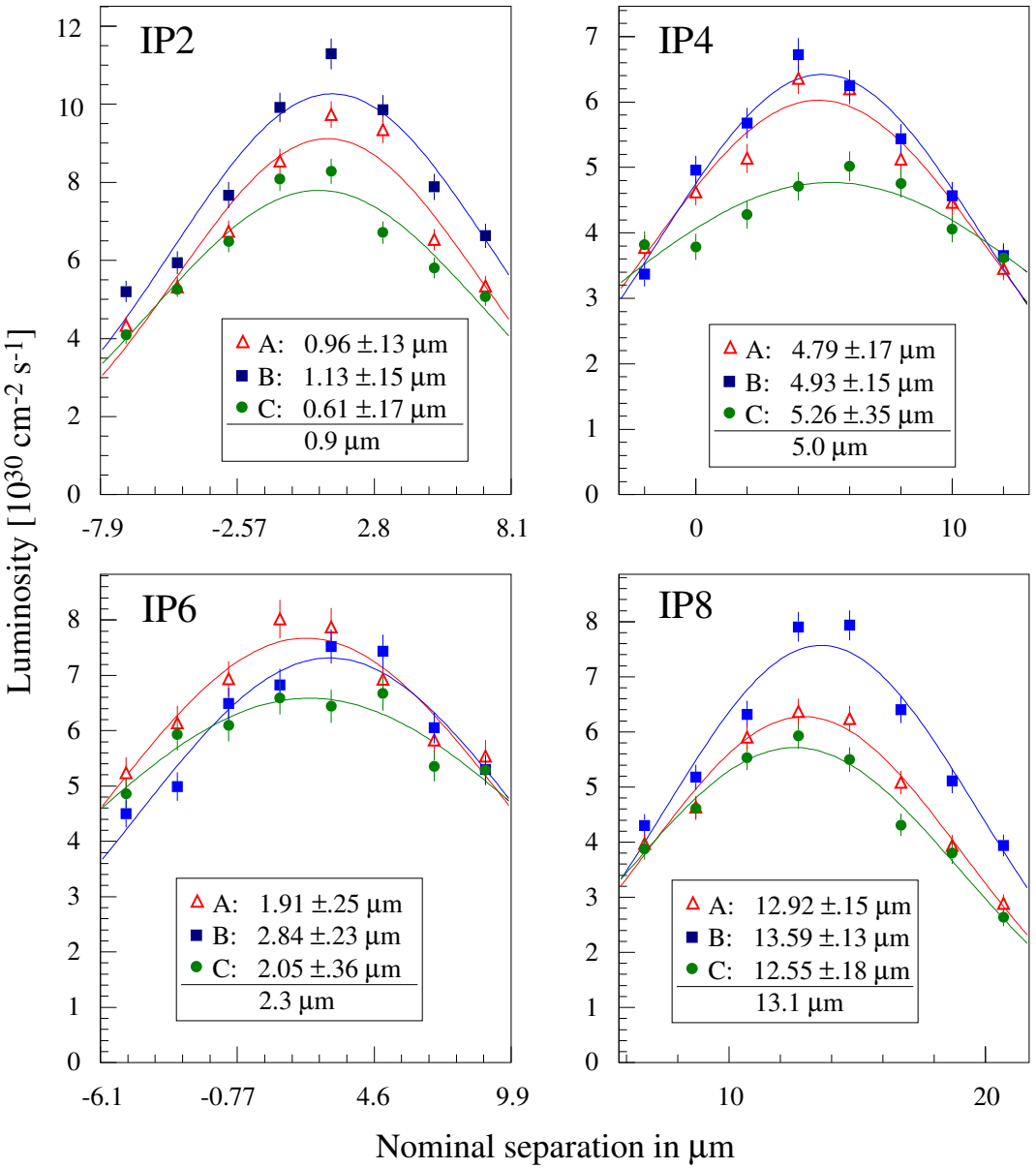

Fig. 9: Example of a luminosity optimization scan at LEP. The luminosity is determined separately for each bunch of a train (labels a,b,c). The optimum setting for the overlap is different for each bunch type.

6 Luminosity optimization

Frequently the primary goal of the machine operation crews is to maximize the luminosity by achieving the best possible overlap of the beams and not necessarily to measure the absolute luminosity. In that case a relative measurement is sufficient. Any process that yields a sufficient rate is acceptable for the luminosity measurement. For e^+e^- colliders Bhabha scattering is the optimum solution, while for hadrons it is possible to monitor the particles that come out of the collision point at small angle. Note that background processes or overlapping events may introduce systematic biases that may have to be taken into account.

An example of luminosity optimization scans at LEP is shown in Fig. 9. The scans were made at each collision point individually. In the example one can observe the luminosity for the three bunches (a,b,c) of a bunch train. The optimum setting is not the same for each bunch owing to parasitic beam–beam deflections: each bunch has a different equilibrium close orbit [19].

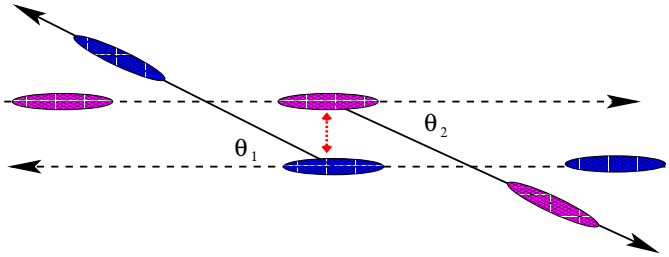

Fig. 10: Coherent deflection of the bunches by the beam–beam force (electromagnetic field) of the counter-rotating bunch

An alternative to the luminosity scan is to use beam position measurements to define the optimum beam overlap. Achieving sufficient accuracy poses tight constraints on position monitor systematic errors (alignment, electronics, etc.) and is usually not sufficient. However, it is possible to define a reference position for the beams using a luminosity scan and then to use this reference to reproduce or stabilize the beam position over longer time intervals.

Continuous optimization may be performed if necessary by changing the separation in small steps. At each step the luminosity is measured and compared with the previous step. If the luminosity is higher, the new position is used as new reference and another step is made in the same direction. If the luminosity is lower, a step in the other direction is performed. This procedure is performed continuously to maintain the highest possible luminosity.

7 The beam–beam deflections

During the beam encounters, the individual particles of each beam are deflected by the electromagnetic field of the counter-rotating beam. When the beams collide with a transverse offset, the bunches may be deflected coherently by the electromagnetic field (beam–beam force) of the counter-rotating bunch (Fig. 10). For e^+e^- circular and linear colliders, the beam–beam deflection may be reconstructed and used to optimize the beam overlap at the collision point. This principle was first used operationally at the SLAC Linear Collider [20] before being used at LEP2 [21].

We consider here the case of flat beams where at the collision point the vertical beam size σ_y is smaller than the horizontal beam size σ_x. It is assumed that the transverse and longitudinal charge distributions of the beams are Gaussian and that the bunch length σ_s is much larger than σ_y and σ_x. As two bunches pass each other, the horizontal and vertical beam–beam kicks $\Delta x'$ and $\Delta y'$ received by a test particle in one bunch due to the electromagnetic field of the counter-rotating bunch are given by [22–25]:

$$\begin{Bmatrix} \Delta x' \\ \Delta y' \end{Bmatrix} = A \begin{Bmatrix} \Im m \\ \Re e \end{Bmatrix} F(x, y, \sigma_x, \sigma_y) \tag{28}$$

where $\Re e$ and $\Im m$ are the real and imaginary parts of the function $F(x, y, \sigma_x, \sigma_y)$:

$$F(x, y, \sigma_x, \sigma_y) = w\left(\frac{x + iy}{\sqrt{2(\sigma_x^2 - \sigma_y^2)}}\right) - e^{-(x^2/2\sigma_x^2 + y^2/2\sigma_y^2)}\, w\left(\frac{x\sigma_y/\sigma_x + iy\sigma_x/\sigma_y}{\sqrt{2(\sigma_x^2 - \sigma_y^2)}}\right) . \tag{29}$$

A is given by

$$A = -\frac{\sqrt{2\pi} N r_e}{\gamma\sqrt{\sigma_x^2 - \sigma_y^2}} \tag{30}$$

where x and y are the horizontal and vertical distances from the test particle to the centre of the counter-rotating bunch; r_e is the classical electron radius; γ is the Lorentz factor; and $w(z)$ is the complex error function.

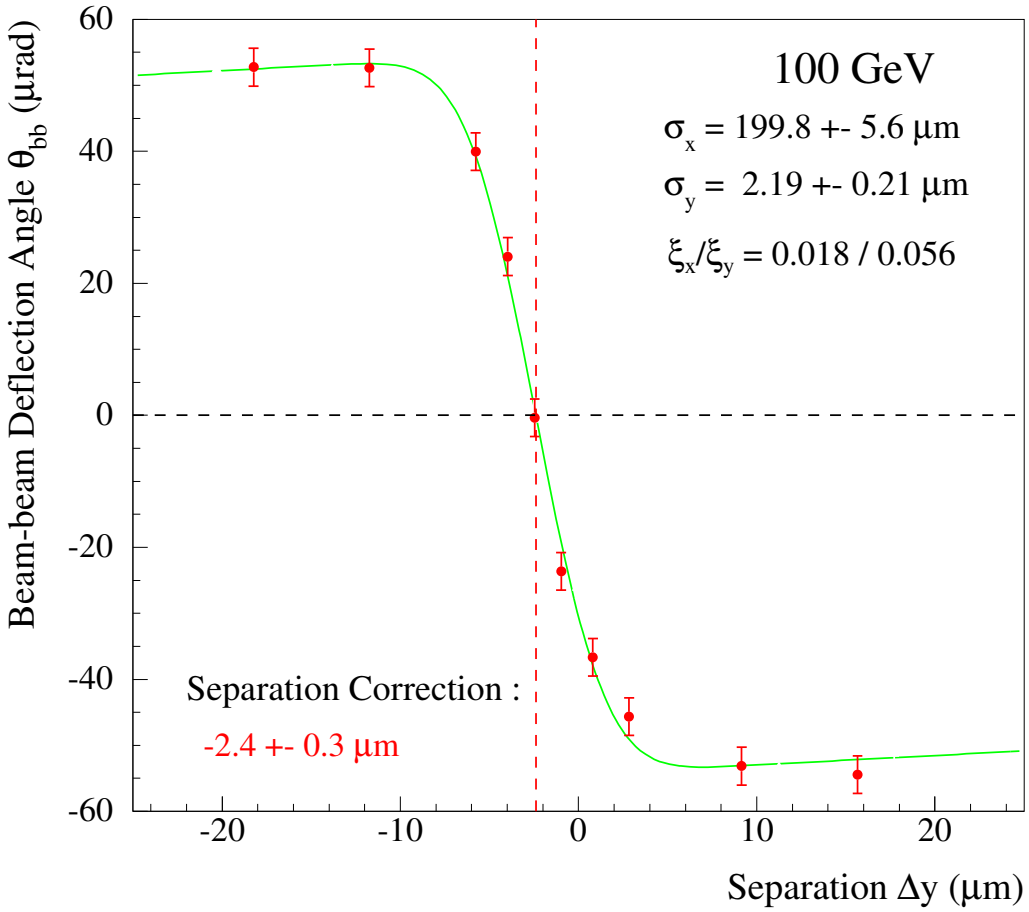

Fig. 11: Example of a vertical plane beam–beam deflection optimization scan at LEP (from Ref. [21]). The beam separation is scanned in a range of ±16 μm which corresponds to 7 to 8 σ_y. The beam size values indicated on the plot are extracted from the fit to the data. ξ_u are the beam–beam tune shifts. At LEP the horizontal beam size was so large that no overlap optimization had to be performed.

For a particle close to the centre of the other bunch, the beam–beam kick increases linearly with the separation ($u = x, y$):

$$\Delta u' = -\frac{4\pi\xi_u}{\beta_u^*}\, u \tag{31}$$

and vanishes when the particle is centred ($u = 0$). The deflection peaks at a separation of a few σ_u before it falls off proportionally to the inverse of the beam separation. The saturation of the deflection is visible in Fig. 11. The betatron function at the collision point is β_u^*. The beam–beam tune shift parameters ξ_u are given by

$$\xi_u = \frac{r_e N \beta_u^*}{2\pi\gamma\sigma_u\,.(\sigma_x + \sigma_y)}\,. \tag{32}$$

The average kick seen by the entire bunch differs from the kick seen by a single particle [24, 25]. It is obtained from Eq. (28) by replacing the beam sizes σ_u with the effective sizes $\tilde{\sigma}_u$:

$$\tilde{\sigma}_u = \sqrt{\sigma_{u,1}^2 + \sigma_{u,2}^2} \tag{33}$$

where 1 and 2 label the two beams. The separations x and y represent the distances between the centres of the two colliding bunches. Since the beam–beam deflection angle is zero is when beams collide without transverse offset, steering the beams to produce no deflection will maximize the luminosity.

To obtain the spatial coordinates of the beams at the collision points, the beam positions must be measured at two beam position monitors (BPM) on each side of the collision point and extrapolated to the collision point with the transfer matrices. To enhance the sensitivity of the measurements, one can take advantage of the fact that the beam–beam kicks are of opposite sign for the two beams. The most sensitive variable is $\theta_{\rm bb}$ which corresponds to the difference of the deflections of the two beams,

$$\theta_{\rm bb} = (\theta^1_{\rm L} - \theta^1_{\rm R}) - (\theta^2_{\rm L} - \theta^2_{\rm R}) \; . \tag{34}$$

Here θ is the beam angle at the collision point, L and R label the left and right sides of the collision point. Depending on the exact configuration, $\theta_{\rm bb}$ may be less sensitive to systematics errors of the BPMs and their electronics because it involves difference measurements. An example for a beam–beam deflection scan performed at LEP is shown in Fig. 11. The deflection $\theta_{\rm bb}$ reaches a few ten's of μrad which can be measured rather easily. At the KEKB B-factory the beam–beam deflection angle is used for a continuous stabilization of the collision point [26].

For undamped hadron beams the beam–beam tune shifts are typically one order of magnitude smaller than for $\rm e^+e^-$ colliders which renders such deflection scans very difficult.

References

[1] F. Ruggiero and F. Zimmermann, *Luminosity optimization near the beam-beam limit by increasing bunch length or crossing angle*, Phys. Rev. ST Accel. Beams **5** (2002) 061001;
B. Muratori, *Luminosity and luminous region calculations for the LHC*, LHC Project Note 301 (2002).

[2] S. van der Meer, CERN internal report ISR-PO/68-31, 1968.

[3] K. Potter, *Luminosity measurements and calculations*, Proc. of the 1984 CERN Accelerator School, CERN 85-19 (Yellow Report), Vol. 2, (1985) pp. 318–30.

[4] K. Potter *et al.*, *Background and luminosity monitoring at the CERN ISR*, Proceedings of PAC 1981, available at the URL `http://accelconf.web.cern.ch/accelconf/`.

[5] S. Jadach *et al.*, *New results on the precision of LEP luminosity*, Acta Phys. Polon. **B30** (1999) 1745–50.

[6] G. DallaValle, *Review of precision determinations of the accelerator luminosity at LEP*, CERN-OPEN-97-002 and Proc. of the 1996 Cracow Symposium on Radiative Corrections.

[7] E. Bravin *et al.*, *Luminosity measurements at LEP*, CERN-SL 97-72 (BI).

[8] V.A. Khoze *et al.*, *Luminosity monitors at the LHC*, Eur. Phys. J. C **19** (2001) 313–22.

[9] M. W. Krasny, J. Chwastowski, K. Slowikowski, *Luminosity measurement method for LHC: the theoretical precision and the experimental challenges*, Nucl. Instrum. Methods Phys. Res. **A584** (2008) 42–52.

[10] LHC Design Report, Volume I, *LHC Main Ring*, CERN-2004-003, Vol. I.

[11] M. Deile *et al.*, *Diffraction and total cross-section at the Tevatron and the LHC*, arXiv:hep-ex/0602021v1.

[12] U. Amaldi *et al.*, *Precision measurement of proton-proton total cross-section at the CERN Intersecting Storage Rings*, Nucl. Phys. **B145** (1978) 367.

[13] M. Bozzo et al., Phys. Lett. **147B** (1984) 5.

[14] TOTEM Collaboration, Technical Design Report, CERN-LHCC-2004-002 (2004).

[15] ATLAS Collaboration, Letter of Intent, *ATLAS forward detectors for luminosity measurement and monitoring*, CERN-LHCC-2004-010 (2004), LHCC-I-014.

[16] A. Faus-Golfe *et al.*, *Luminosity determination using Coulomb scattering at the LHC*, Proceedings of EPAC 2002, Paris, France, available at the URL `http://accelconf.web.cern.ch/accelconf/`.

[17] A.J. Baltz, C. Chasman and S.N. White, *Correlated forward–backward dissociation and neutron spectra as luminosity monitor in heavy ion colliders*, Nucl. Instrum. Methods Phys. Res. **A417** (1998) 1.

[18] C. Adler *et al.*, *The RHIC zero degree calorimeter*, Nucl. Instrum. Methods Phys. Res. **A470** (2001) 488–99.

[19] D. Brandt, H. Burkhardt, M. Lamont, S. Myers and J. Wenninger, *Accelerator physics at LEP*, Rep. Prog. Phys. **63** (2000) 939-1000, [CERN-SL-2000-037 DI].

[20] P. Bambade *et al.*, Phys. Rev. Lett. **62** (1989) 2949.
W. Koska *et al.*, Nucl. Instrum. Methods Phys. Res. **A286** (1990) 32.

[21] J. Wenninger *et al.*, *Luminosity optimization using beam–beam deflections at LEP*, Proceedings of EPAC 1996, Sitges, Spain, available at `http://accelconf.web.cern.ch/accelconf/`.

[22] M. Basseti and G.A. Erskine, CERN-ISR-TH/ 80-06 (1980).

[23] R. Talman, AIP Conference Proc. **153** (1987) 789.

[24] K. Hirata, Nucl. Instrum. Methods Phys. Res. **A269** (1988) 7.

[25] E. Keil, *Beam–beam dynamics*, CERN SL/94-78 (1994).

[26] Y. Funakoshi *et al.*, *Orbit feedback system for maintaining an optimum beam collision*, Phys. Rev. ST Accel. Beams **10** (2007) 101001.